Control of Unidirectional Transport of Single-File Water Molecules through Carbon Nanotubes in an Electric Field

Jiaye Su and Hongxia Guo*

Beijing National Laboratory for Molecular Sciences, Joint Laboratory of Polymer Sciences and Materials, State Key Laboratory of Polymer Physics and Chemistry, Institute of Chemistry, Chinese Academy of Sciences, Beijing 100190, China

ABSTRACT The transport of water molecules through nanopores is not only crucial to biological activities but also useful for designing novel nanofluidic devices. Despite considerable effort and progress that has been made, a controllable and unidirectional water flow is still difficult to achieve and the underlying mechanism is far from being understood. In this paper, using molecular dynamics simulations, we systematically investigate the effects of an external electric field on the transport of single-file water molecules through a carbon nanotube (CNT). We find that the orientation of water molecules inside the CNT can be well-tuned by the electric field and is strongly coupled to the water flux. This orientation-induced water flux is energetically due to the asymmetrical water−water interaction along the CNT axis. The wavelike water density profiles are disturbed under strong field strengths. The frequency of flipping for the water dipoles will decrease as the field strength is increased, and the flipping events vanish completely for the relatively large field strengths. Most importantly, a critical field strength E_c related to the water flux is found. The water flux is increased as E is increased for $E \leq E_c$, while it is almost unchanged for $E > E_c$. Thus, the electric field offers a level of governing for unidirectional water flow, which may have some biological applications and provides a route for designing efficient nanopumps.

KEYWORDS: water molecule · transport · carbon nanotube · electric field · molecular dynamics simulation

Water as a key constituent in cell biology[1] has some unusual physical and chemical properties, such as its potency as a solvent, its ability to form hydrogen bonds, and its amphoteric nature. In a broad sense, water is not only the matrix of life but also the matrix of the world and of all its creatures. It is well-recognized that the structures and thermodynamic properties of water in nanotubes (or channels) are fundamentally different from bulk water. Examples include nonpolar cavities in proteins,[2,3] fullerenes,[4−6] and two hydrophobic plates[7−13] or single hydrophobic/hydrophilic walls.[14−16] In particular, when confined in nanopores, water can form unique ordered ice or solid-like structures,[17−20] and thereby exhibits anomalous diffusion or transport behavior.[21−23] Generally, confined water molecules would like to form hydrogen-bonded wires or clusters.[24] These unusual properties of water in nonpolar confinement are also relevant to the design of novel nanofluidic devices, such as molecular sieves,[25−27] novel desalination machines,[28−31] fuel cells,[32−35] drug delivery,[36,37] as well as biosensors.[38−40]

In addition, the transport of water molecules through nanometer water channels plays an important role in biological activities.[41−47] Croot and Grumuller[48] first observed single-file water chains when they used molecular dynamics (MD) simulations to study the translocation of water molecules across the biological membrane proteins, aquaporin-1 (AQP1) and Glpf. Furthermore, Zhu *et al.* investigated the osmotic permeability of Glpf[49] and AQP1[50] using a technique of artificial osmotic pressure in their MD simulations. Despite extensive studies on water transport through biological channels or nanopores,[41−50] the knowledge of the effects of the shape or dimension of biological pores and external fields on the behavior of water molecules is still missing. In light of the unique properties of single-file water chains, a deeper understanding of the detailed molecular mechanism is instrumental in exploiting the primary characters of the biological channels.[41]

Actually, considerable attention has been paid to the structures and dynamics of single-file water molecules.[21−24,28,29,32,33,39,41,47−50] As a pioneering work, in 2001 Hummer and coworkers[51] reported the fast conduction ability of a short carbon nanotube solvated in a water box by using MD simulations, where the water molecules inside the CNT were in single-file. They further discussed the effect of water−nanotube interactions on the

*Address correspondence to hxguo@iccas.ac.cn.

Received for review June 28, 2010 and accepted December 10, 2010.

Published online December 16, 2010. 10.1021/nn1014616

water occupancy.[52] They also suggested that the rapid water flow was related to the weak attractions between water and confining walls, as well as the strong interactions between water molecules.[24] As a result, the water flow rate can even exceed expectations from macroscopic hydrodynamics by several orders of magnitude.[24] Interestingly, in 2006, Holt *et al.*[53] experimentally observed the enhanced water flow through carbon nanotubes. They found that the water flow rate through a carbon nanotube with a radius of 1 to 2 nm was about a factor of 3 orders of magnitude faster than the conventional nonslip hydrodynamic flow. Meanwhile, by the use of MD simulation, Joseph and Aluru[54] addressed the enhanced flow rate arising from a velocity "jump" in the depletion region at the water−nanotube interface. They demonstrated that the water orientations and hydrogen bonds at the interface could increase the flow rate remarkably. Therefore, if such carbon nanotubes can be used for seawater desalination,[28−31] the energy required will be significantly reduced.

On the other hand, the pressure-driven transport of single-file water molecules could be well-controlled by an external charge outside the carbon nanotube[55] or by the deformation of the CNT.[56] In a series of original work, Aluru *et al.* demonstrated that the water flux and transport dynamics are dominated by many factors including pore charges,[57] electric field induced by biomolecules,[58] composition of nanotubes,[59] and so forth. More importantly, the single-file behavior of water molecules inside the CNTs is relevant to pumping efficiency. For example, in a recent MD simulation,[60] Gong *et al.* presented a design of a molecular water pump by using a combination of charges positioned adjacent to a carbon nanotube according to the charge distribution in biological water channels, AQPs. On the contrary, with the same model,[61] Zuo *et al.* observed that the water flux was about 1 order of magnitude smaller than the value reported in Gong's work. It was shown that,[61] as in the aquaporins, asymmetrically positioned charges could not generate robust unidirectional water flow across the carbon nanotube, which was also confirmed by our MD simulations. Thus, the model designed by Gong *et al.* should be more appropriate as a biomimicking water channel rather than a pump.[61]

Though great effort and progress[47−61] has been made, it is still difficult to achieve a controllable and unidirectional water flow. Wan *et al.*[62] have demonstrated that the dependence of water flux on the dipole orientation of water molecules inside nanopores is remarkable such that a considerable net flux along the dipole orientation is observed. In fact, the orientation of water dipole could be tuned more easily by external electric fields when water molecules are confined either between two hydrophobic plates[12,13] or in nanopores.[63] In a recent exciting MD simulation,[64] Joseph and Aluru used an electric field to drive water molecules through 9.83 nm long CNTs, where a net water flux along the dipole orientation was first observed. They ascribed the pumping events to the rotation−translation coupling, and the intrinsic physical mechanism was explored. However, knowledge of the dependence of water flux, dipole orientation, and frequency of flipping on the electric field, as well as the coupling between water dipole orientation and flux, is still lacking. These fundamental problems are essential for understanding the underlying mechanism of the biased transport of single-file water chains and for designing novel nanofluidic devices with high flux and selectivity. Up to now, there have been few simulations systematically dealing with these issues, which inspire further studies toward this direction.

To this end, in the present work, we systematically investigate the effect of electric field on the transport of single-file water molecules through a short carbon nanotube that has been extensively studied.[51,55,56,62] We focus on the dependence of water transport dynamics, such as dipole orientation, water flux, flipping frequency, and otherwise on field strengths. From this point of view, our present work could be seen as a further extension of the study by Joseph and Aluru.[64] The electric field is applied along the tube axis, and we vary the values between $E = 0.01$ and 1.0 v/nm, which is within the range of typical field strengths in ion channels or membranes.[12,13] In order to obtain a reliable value for water flow, we conduct three independent 410 ns MD simulations for each value of E, and the last 400 ns is used for data analysis. We show that the dipole orientation of water molecules inside the CNT can be well-controlled by the electric field. Though the water flow in such a short CNT is in bursts,[51,52] a considerable net flux is observed along the dipole orientation. We also find that such a concerted dipole orientation will result in an asymmetric potential of water−water interaction along the tube axis, which is in agreement with Wan *et al.*[62] The dependence of density profiles along the tube axis and the frequency of flipping on the electric field are also explored. Significantly, a critical field strength related to the maximum water flux is detected. Therefore, our results will reveal some new insights different from Joseph's work,[64] and to some extent, a controllable and unidirectional water transportation could be achieved by the electric field. These findings can not only help us to understand the biased transport of single-file water molecules but also be useful for designing novel controllable water nanopumps.

RESULTS AND DISCUSSION

In the present study, an uncapped armchair single-walled carbon nanotube with a length of 1.34 nm and a diameter of 0.81 nm was used, which has been extensively adopted by previous work.[51,52,55,56,62] In experiment, carbon nanotubes have shown unique electrical, optical, and mechanical properties[65−67] and have been extensively utilized in nanotechnology. In order to

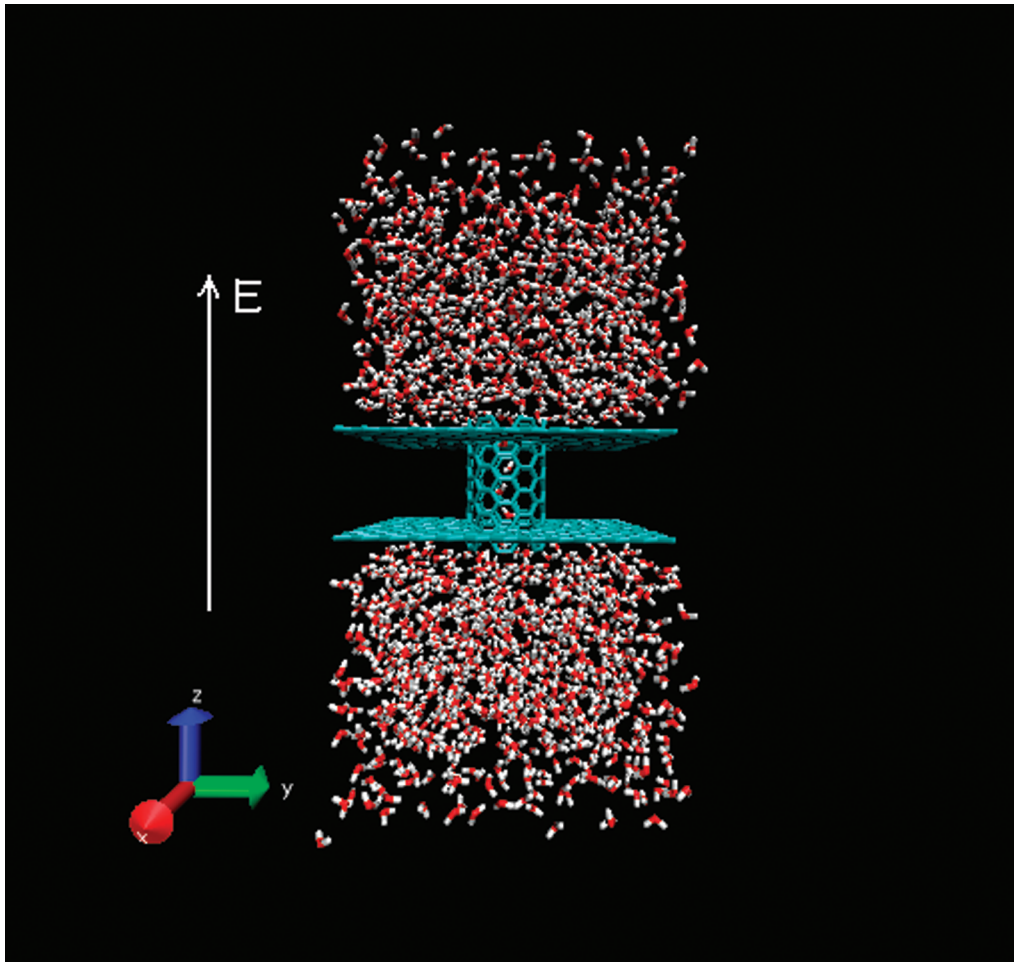

Figure 1. Snapshot of the simulation system. The (6,6) type CNT combined with two graphite sheets is solvated in a water box of 3 × 3 × 6 nm^3 with 1481 molecules. The axis of CNT is parallel to the *z*-axis, and the external electric field is also applied in the *z*-axis direction.

mimic biological channels in a membrane, the CNT was embedded between two graphite sheets along the *z*-axis, as illustrated in Figure 1. The CNT combined with two graphite sheets divided the water box into two equal parts. Consequently, the center of the CNT was the center of the whole simulation box. For convenience, we shifted the CNT center to the position of $x = 0$ nm, $y = 0$ nm, and $z = 0$ nm. The external electric field was applied along the *z*-axis, and the screening effect by the CNT[64] was not considered here. The carbon atoms were modeled as uncharged Lennard-Jones particles with parameters taken from ref 51. The TIP3P water model[68] was used.

The major goal of the present study is to explore the detailed molecular level mechanism responsible for biased transport of single-file water molecules through carbon nanotubes. In order to understand the structures and orientations of such single-file water chains inside the CNT, we first investigate the average dipole orientations at different field strengths. Figure 2a gives the distributions of the averaged dipole orientation of water molecules inside the carbon nanotube for various values of *E*. Here, θ represents the angle between a water dipole (defined from the oxygen atom to the center of two hydrogen atoms) and the tube axis, and the average is taken over all water molecules inside the CNT. Note that, in our studied *E* values, $\langle\theta\rangle$ mostly lies between two ranges of 10−50 and 130−170°, quite in agreement with previous studies.[55,56,62] It has been demonstrated that the single-file water molecules are highly oriented with the averaged dipole orientations either nearly along or opposite to the tube axis, and they collectively flip directions within a duration of 2−3 ns.[51,62] For $E = 0$ v/nm, the two peaks are almost symmetric with respect to $\langle\theta\rangle = 90°$. For convenience, we define $0 < \langle\theta\rangle < 90°$ as +dipole states, while $90° < \langle\theta\rangle < 180°$ as −dipole states. We find that the two peaks become more asymmetric with increasing *E*, and the +dipole states are more preferred to the −dipole states, which is again in good agreement with Vaitheeswaran's theoretical predictions.[63] At $E = 0.1$ v/nm, the −dipole states almost disappear. Remarkably, for strong field strength of $E = 1.0$ v/nm, the peak position shifts to 20° instead of about 30° for $E = 0-0.1$ v/nm. To further explore the dependence of +dipole or −dipole states on the field

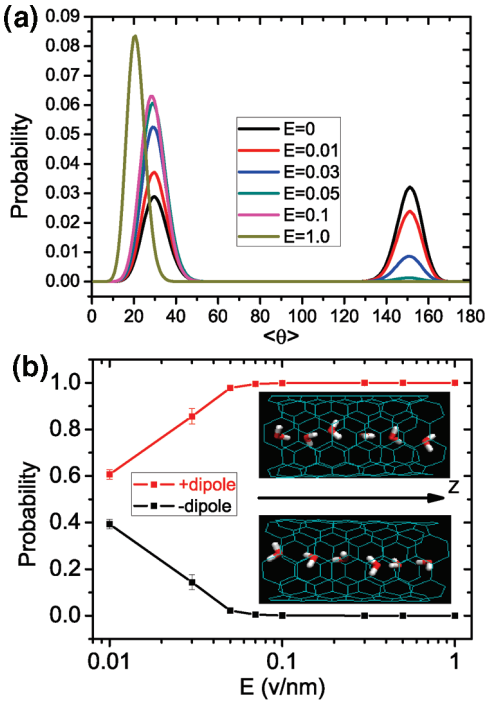

Figure 2. Water dipole orientation inside the CNT. (a) Probability distributions of the averaged dipole orientation of water molecules inside the CNT, $\langle\theta\rangle$ for $E = 0$, 0.01, 0.03, 0.05, 0.1, and 1.0 v/nm. (b) Probabilities of the +dipole and −dipole states as a function of E. The standard error bars (in this figure and following) are shown for three independent 410 ns MD runs and for clarity are not shown in some figures.

strength, we also calculated their probabilities as a function of E, as presented in Figure 2b. For the three independent 410 ns MD simulations, the probabilities of +dipole and −dipole are close to each other for $E = 0$ v/nm, whose values are 0.475 ± 0.044 and 0.525 ± 0.044, respectively. The probabilities for +dipole increase remarkably as E is increased from 0.01 to 0.1 v/nm, while the opposite trend is observed for the −dipole. For $E = 0.1-1.0$ v/nm, the orientation of water molecules inside the CNT is completely controlled by the electric field.

To further illustrate the effect of electric field on the water transport, we show in Figure 3 the resulting net water flux as well as the water occupancy. Without loss of generality,[51,55,56,61,62] we define the upflux/downflux as the total number of water molecules per nanosecond conducted through the CNT from bottom/top (−z/+z) to top/bottom (+z/−z), respectively. The flow is the sum of upflux and downflux, while the flux is the difference between them. During the total simulation time of 1230 ns (1200 ns in data collection), we observed 19 009 water molecules conducted through the CNT for $E = 0$ v/nm, resulting in a flow of 15.84 ± 0.26 ns^{-1}, quite in agreement with the value of 17 ns^{-1} in ref 51. Interestingly, as seen in Figure 3, the net water flux increases with increasing E for $E < 0.07$ v/nm and maintains 1.1−1.2 ns^{-1} for $E \geq 0.07$ v/nm, which is 4 times larger than the value of ~0.28 ns^{-1} in the biomimicking water channel.[61] We also note that the flux of 1.2 ns^{-1} is comparable to the experimental value of 1.8 ns^{-1} in aquaporin channels.[69,70] This phenomenon indicates that the electric field may be an appropriate choice for biological water channels to achieve rapid water transportation with high selectivity. In particular, the maximum field strength of 1.0 v/nm used here is still within the range of recent experimental values.[71]

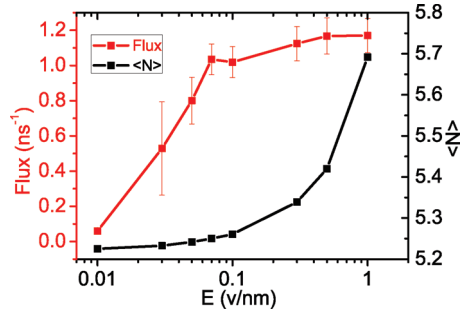

Figure 3. Averaged water flux through the CNT as well as the average occupancy of water molecules inside the CNT $\langle N\rangle$ with respect to the electric field E.

Furthermore, we found that there was a strong coupling between the water flux and dipole orientation. As seen in Figure 2b, the probability of +dipole states attains 0.995 ± 0.005 at $E = 0.07$ v/nm, where the water flux reaches its maximum value. Thus, a maximum flux is suggested to be achieved when the probability of +dipole states is larger than about 0.99. Li and Wan *et al.* showed that the water flux induced by osmotic pressure could be well-controlled by a charge outside the CNT[55] or the deformation of the CNT.[56] Similarly, the water flux herein can also be well-tuned by the electric field. On the basis of these results, we can conclude that the water dipole orientation inside the CNT can be well-controlled by the electric field, resulting in a controllable net water flux, which may provide some new insights compared with the study by Joseph and Aluru.[64] The observed mechanism can offer useful insights into the design of a controllable water nanopump and novel biological water channels.

The filling of nonpolar cavities or nanopores in proteins and biological water channels[2,3,24] can be well-described by the water occupancy. As seen in Figure 3, the average occupancy $\langle N\rangle$ increases monotonously from 5.225 ($\pm 4.8 \times 10^{-4}$) to 5.692 ($\pm 3.1 \times 10^{-4}$) as E is increased from 0.01 to 1.0 v/nm, which agrees well with the theoretical analysis by Vaitheeswaran *et al.*[63] Actually, the increase of $\langle N\rangle$ is very slow for $E =$ 0.01−0.1 v/nm, while it becomes remarkable for strong field strength of $E = 0.1-1.0$ v/nm. The free energy of occupancy fluctuations can help us to understand the emptying−filling transitions of nanotubes, which further captures key properties of light sensors as single-molecule field-effect transistors for protonic currents.[51] The free energy of occupancy fluctuations $G(N)$ is also calculated and shown as a function of N for different E in Figure 4. Note that $G(N) = -k_BT \ln p(N)$, where $p(N)$ is

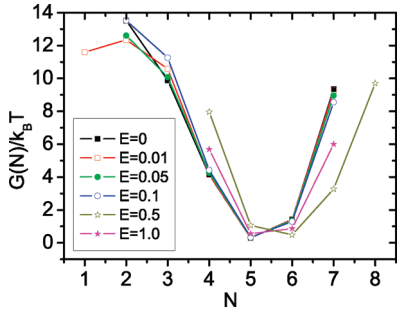

Figure 4. Free energy of occupancy fluctuations $G(N) = -k_BT$ ln $p(N)$ for $E = 0$, 0.01, 0.05, 0.1, 0.5, and 1.0 v/nm. Note that probabilities of occupancy $P(N)$ are averaged from the three 410 ns MD runs.

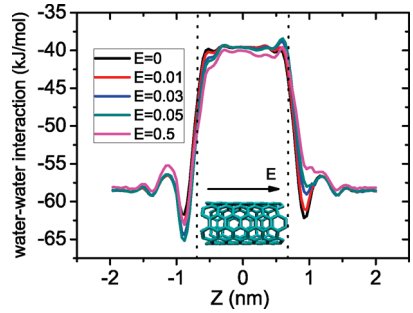

Figure 6. Water−water interaction as a function of a water position for $E = 0$, 0.01, 0.03, 0.05, and 0.5 v/nm. Note that the interaction becomes asymmetric as E is increased. The two dotted lines represent the positions of the inlet and outlet of the CNT.

the probability of finding exactly N water molecules inside the CNT.[51] As shown in Figure 4, the free energy $G(N)$ curves for $E = 0.01-0.1$ v/nm are very similar to the case of $E = 0$, while the location of valley shifts from $N = 5$ to $N = 6$ as E is increased to 1.0 v/nm, in accordance with the results of $\langle N \rangle$. In fact, $N = 5$ and $N = 6$ are the most preferable two states for all of the cases in our studied length of nanotube. For the free case of $E = 0$, the precise value of valley should depend on CNT lengths, just as Waghe *et al.* showed that longer CNTs were occupied by more water molecules.[52]

In order to understand the flipping of water dipoles inside the CNT and its sensitivity to the electric field, we also calculated the average angle $\langle \theta \rangle$ as a function

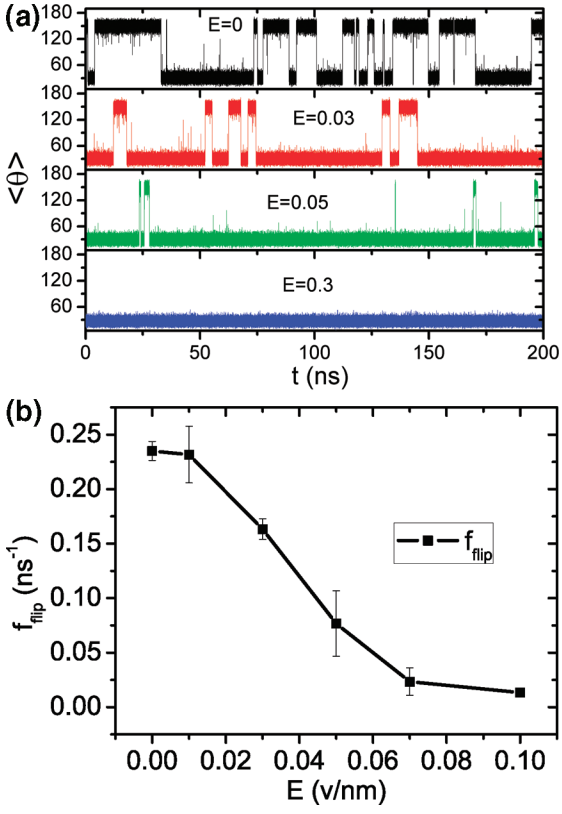

Figure 5. (a) Evolution of $\langle \theta \rangle$ with respect to simulation time for $E = 0$, 0.03, 0.05, and 0.5 v/nm. (b) Dependence of flipping frequency f_{flip} on the electric field.

of simulation time for different E. As shown in Figure 5a, for $E = 0$ v/nm, $\langle \theta \rangle$ flips between +dipole and −dipole states frequently, and the average durations for the two states are comparable. When E is increased, the flipping frequency decreases remarkably, and the average duration of −dipole states becomes short-lived and vanishes for $E = 0.3$ v/nm. Meanwhile, a flip can be defined as $\langle \theta \rangle$ passing through 90°, and thus we can compute the average flipping frequency, f_{flip}, shown as a function of E in Figure 5b. During the 1200 ns collection time, 282 flips are observed for $E = 0$ v/nm, corresponding to a flipping frequency of $f_{flip} = 0.235 \pm 0.009$ ns^{-1} or a flipping period of $\tau_{flip} = 1/f_{flip} = 4.26 \pm 0.16$ ns, well within the range of 4−6 ns measured in ref 72. A duration of 2−3 ns is also observed for the same CNT with different structures outside.[51,62] In particular, Kofinger *et al.*[73] demonstrated that the flipping period can be even up to ~0.1 s for a tube with a macroscopic length of ~0.1 mm. Generally, f_{flip} is governed by the potential barrier against flipping. As the strength of electric field is increased, the orientation of water molecules inside the CNT favors along the field direction, and thus the flipping events should be reduced significantly.[52] As seen, the average flipping frequency f_{flip} in Figure 5b decreases monotonously with increasing E, and no flips can be observed for $E \geq 0.3$ v/nm. It is worth noting that τ_{flip} is not a suitable quantity to characterize the average duration of +dipole or −dipole states for our studied field strengths. For instance, there are total 16 flips for $E = 0.1$ v/nm, therefore, $\tau_{flip} \sim 75$ ns. The average duration of +dipole states is about $2\tau_{flip}$, while the durations of corresponding eight −dipole states are as short as only 0.5, 1.5, 0.5, 1.5, 1.5, 0.5, 0.5, and 1439.5 ps, respectively. Notwithstanding, for all cases, the quantity f_{flip} can accurately measure the frequency of flipping.

The water flux is related to the strong interactions between water molecules. To explore the mechanism, we also calculated the water−water interaction as a function of water position along the CNT axis for different E, shown in Figure 6. The two dotted lines mark the positions of the inlet and outlet of the CNT, respec-

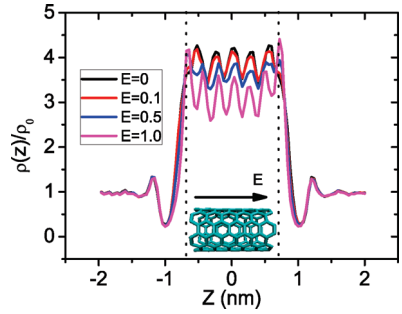

Figure 7. Water density profiles along the CNT axis for E = 0, 0.1, 0.5, and 1.0 v/nm; ρ_0 is the density of bulk water and is considered as 1.0 g/cm^3. The two dotted lines represent the positions of the inlet and outlet of the CNT.

tively. For the free case of $E = 0$ v/nm, the water−water potential is highly symmetric with respect to the tube center of $z = 0$. As E is increased, the potential becomes more and more asymmetric, not only for the water position inside the tube but also for the positions in the two vestibules of the inlet and outlet. In fact, such an asymmetric water−water interaction results from the single-file water chain with a concerted dipole orientation. A water molecule should sacrifice its rotational freedom as well as on average two out of four hydrogen bonds to enter the CNT. For the +dipole state typically shown in the inset in Figure 2b, the two hydrogen atoms of each water molecule inside the CNT face the $+z$ reservoir as well as oxygen atoms face the $-z$ reservoir, leading to the asymmetric water−water potentials. Without external fields, Wan *et al.*[62] considered the +dipole and −dipole states separately and observed the asymmetric water−water potentials. They attributed the net water flux to the asymmetric water−water interaction inside the tube. We expect that the two asymmetric potential valleys in the vestibules for $E > 0$ v/nm are also related to the water flux. As one can see from Figure 6, in the $+z$ vestibule, the potential valley becomes smaller as E is increased, thus it is a little difficult for water molecules to enter the CNT from the $+z$ reservoir. The potential valley in the $-z$ vestibule ensures the permeation of water molecules from the $-z$ reservoir into the $-z$ entrance of the CNT. Therefore, it becomes easier for water molecules to transport through the CNT from $-z$ to $+z$.

Figure 7 shows the water density distributions $\rho(z)$ along the tube axis for different values of E, where ρ_0 is the bulk density and is considered as 1.0 g/cm^3. The wavelike patterns with five similar peaks for $E = 0$ are in excellent agreement with previous studies,[51] implying the unique arrangement of water molecules inside the CNT. This wavelike density profile induced by the tight bonding network inside the nanochannel is directly related to the ice or solid-like properties of confined water and may have potential applications in mass storage.[24,41] Also, there are two valleys with low densities in the vestibules, which are related to the fast exchange of water molecules between the channel and the two reservoirs. For weak field strengths of E = 0.01−0.1 v/nm, no obvious variations in the density are observed. However, the wavelike patterns are disturbed remarkably for $E = 0.5$ and 1.0 v/nm. Two additional peaks at the inlet and outlet of the CNT are detected clearly for $E = 1.0$ v/nm. Due to the strong hydrogen bond network in bulk water, the structural and dynamical properties of water molecules outside the channel are less susceptible to the electric field. In contrast, inside the channel not only the filling but also the structure of water molecules is appreciably affected by the electric field. By evaluating the grand-canonical partition function, Vaitheeswaran *et al.* have shown that homogeneous electric fields favor the filling of previously empty nanotubes with water from the bulk phase.[63] The tendency of average water occupancy in Figure 3 agrees well with their theoretical predictions, and the most probable state is $N = 6$ for $E = 1.0$ v/nm instead of $N = 5$ according to Figure 4. In addition, the most probable angle $\langle\theta\rangle$ is 20° for $E = 1.0$ v/nm, while it is about 30° for $E = 0$−0.1 v/nm. Therefore, the water molecules inside the CNT will reorganize their correlated single-file structures to accommodate the strong electric field, resulting in biased density profiles.

It is known that the water density distribution is related to the potential of mean forces (PMFs) by $F(z) = -k_BT \ln[\rho(z)/\rho_0]$.[61] The PMF is often used to characterize the behavior of water molecules inside the channel. The wavelike density distributions in Figure 7 will directly lead to wavelike patterns of PMFs, triggering burst-like water flows.[51] It is clear that the large fluctuation of peaks and valleys in the density profile for E = 1.0 v/nm can energetically favor the filling of water molecules, in accordance with the results of $\langle N\rangle$.

CONCLUSIONS

In summary, we have systematically investigated the effect of electric field on the transport of single-file water molecules through a short carbon nanotube by using extensive molecular dynamics simulations. Of particular interest is that a controllable net water flow can be achieved to some extent by applying an electric field along the tube axis and is strongly coupled to the water dipole orientation inside the channel. It should be noted that water molecules cannot completely transport along the direction of water dipoles or the electric field. The net water flux energetically results from the asymmetric water−water interactions. The flipping frequency f_{flip} will decrease as the field strength increases and the flipping events vanish completely for $E \geq 0.3$ v/nm. Actually, only in the free case of $E = 0$ v/nm can $\tau_{flip} = 1/f_{flip}$ represent the average duration of +dipole or −dipole states. However, for all the cases of E = 0−1.0 v/nm, the quantity f_{flip} could just denote the frequency of flipping. The density profiles along the tube axis, which are related to the potential of mean force, are disturbed by a strong applied field of $E \sim 0.5$ v/nm,

showing the tendency for electric field to facilitate the filling of the CNT, in good agreement with Vaitheeswaran's theoretical prediction.[63] Most significantly, the resulting water flux can be well-controlled by the electric field with a critical field strength of $E_c \sim 0.07$ v/nm, which offers a possible route to reduce the energy needed for nanopump devices. These findings help us to understand the biased transport of single-file water molecules, which could be applicable in biological channels[48−50,69,70] and useful for designing efficient nanofluidic machines. Indeed, if the water molecules in biological or artificial nanochannels are in single-file, the electric field may be an appropriate choice to achieve net water flux.

Although the present results are based on a short carbon nanotube, the main conclusions are expected to be maintained for longer nanopores with similar radius, as Joseph and Aluru[64] have previously shown that the water dipoles in 9.83 nm CNTs can also be completely controlled by the two studied field strengths of $E = 0.1$ and 1.0 v/nm. To consider this issue simply, we have also conducted 410 ns MD simulations for a twice longer CNT (2.63 nm in length and same radius) at several field strengths of $E = 0.03$, 0.05, 0.07, and 0.1 v/nm. During the 410 ns simulation, for all of the four field strengths, the water dipole orientation inside the CNT is almost maintained along the field direction (except for a little deviation of $E = 0.05$ v/nm). It is known that the frequency of flipping will decrease considerably as the CNT length increases[62,73] since the potential barrier against flipping is increased. Therefore, it needs relatively low field strengths to control the dipole orientation for longer CNTs. The dipole orientation will become more sensitive to the external field, and the critical field strength is expected to be decreased. Meanwhile, it becomes difficult for us to investigate the dependence of dipole orientation, water flux, flipping frequency, and so forth on the field strength for long CNTs at given available simulation times of hundreds of nanoseconds. Especially, extremely long simulation runs with a notable expense of computational resources are required to determine the critical field strength and further to make similar observations as those for the present short CNT. That is probably a part of the reason for us to choose a widely used short CNT for the present study.

The similar asymmetric water−water interaction for the longer CNT is also observed. Interestingly, though, the total water flow is decreased remarkably compared to the shorter CNT, a comparable water flux is observed. Take $E = 0.1$ v/nm as an example, the water flux/flow are 1.02/15.65 and 1.40/2.32 ns^{-1} for the shorter and longer CNTs, respectively. Moreover, if we define η = flux/flow as a unidirectional transport efficiency, we can find that the efficiency for the longer CNT ($\eta = 60.3\%$) is much larger than the shorter one ($\eta = 6.5\%$). This finding may also be helpful for the choice of CNT lengths for designing efficient nanopumps. It is expected that, given the water dipole orientation inside short CNTs is completely kept along the field direction, a large amount of water molecules can still move against the field direction due to the competition between thermal fluctuations (mainly contributed from the two reservoirs) and the asymmetric water−water interactions. For long CNTs, the thermal fluctuation can be effectively screened by the CNTs, as the distance from the water molecules inside the CNT to those in the two reservoirs is close to or larger than the cutoff, and hence water molecules are driven along the field direction more easily by the asymmetric water−water interactions or by the rotation−translation coupling.[64] As a result, the pump efficiency may increase as the CNT length increases, but further extensive studies are needed to identify the quantitative relationships.

In a word, our results present quantitative dependence of water dipole orientation, flux, flipping frequency, and so forth on the electric field, suggesting a controllable nanopump for water, which may reveal some new insights different from ref 64. At the same time, several issues still remain unsolved after the present study. For instance, the dependence of critical field strength and pump efficiency on the CNT length is still unknown. Also, without an external electric field, previous works on the effect of nanopore radius showed that for the larger radius the unique ice or solid-like water structure is preferred instead of the single-file one,[17−21] but the study of an applied field in these cases is lacking. With the increase of computational resources, further extensions of this work may be motivated toward these problems.

METHODS

All MD simulations were carried out at constant pressure (1 bar with an initial box size of $L_x = 3.0$ nm, $L_y = 3.0$ nm, $L_z = 6.0$ nm) and temperature (300 K) using the Berendsen method for pressure coupling and the Nosé−Hoover method for temperature coupling with Gromacs 3.3.1 simulation package.[74] The TIP3P water model[68] was used. The carbon−carbon and carbon−water interaction parameters were taken from ref 51. The carbon nanotube combined with two graphite sheets were held fixed during the simulations. The van der Waals interactions were calculated with a cutoff (10 Å). The particle-mesh Ewald method[75] was used to treat the long-range electrostatic interactions. Periodic conditions were applied in all directions. A time step of 2 fs was used, and data were collected every 0.5 ps. In order to obtain reliable data for water flow, we extended the simulation time for each value of electric field up to 410 ns, and the last 400 ns was used for data analysis. Moreover, three independent MD runs were conducted, and thus the total simulation time for each field strength was up to 1230 ns.

Acknowledgment. This work is financially supported by Chinese Academy of Sciences (KJCX2-YW-H19).

REFERENCES AND NOTES

1. Ball, P. Water as an Active Constituent in Cell Biology. *Chem. Rev.* **2008**, *108*, 74–108.
2. Yin, H.; Hummer, G.; Rasaiah, J. C. Metastable Water Clusters in the Nonpolar Cavities of the Thermostable Protein Tetrabrachion. *J. Am. Chem. Soc.* **2007**, *129*, 7369–7377.
3. Collins, M. D.; Hummer, G.; Quillin, M. L.; Matthews, B. W.; Gruner, S. M. Cooperative Water Filling of a Nonpolar Protein Cavity Observed by High-Pressure Crystallography and Simulation. *Proc. Natl. Acad. Sci. U.S.A.* **2005**, *102*, 16668–16671.
4. Iwamatsu, S.; Uozaki, T.; Kobayashi, K.; Re, S. Y.; Nagase, S.; Murata, S. A Bowl-Shaped Fullerene Encapsulates a Water into the Cage. *J. Am. Chem. Soc.* **2004**, *126*, 2668–2669.
5. Ramachandran, C. N.; Sathyamurthy, N. Water Clusters in a Confined Nonpolar Environment. *Chem. Phys. Lett.* **2005**, *410*, 348–351.
6. Vaitheeswaran, S.; Yin, H.; Rasaiah, J. C.; Hummer, G. Water Clusters in Nonpolar Cavities. *Proc. Natl. Acad. Sci. U.S.A.* **2004**, *101*, 17002–17005.
7. Giovambattista, N.; Rossky, P. J.; Debenedetti, P. G. Effect of Pressure on the Phase Behavior and Structure of Water Confined between Nanoscale Hydrophobic and Hydrophilic Plates. *Phys. Rev. E* **2006**, *73*, 041604.
8. Leung, K.; Luzar, A.; Bratko, D. Dynamics of Capillary Drying in Water. *Phys. Rev. Lett.* **2003**, *90*, 065502.
9. Lum, K.; Chandler, D.; Weeks, J. D. Hydrophobicity at Small and Large Length Scales. *J. Phys. Chem. B* **1999**, *103*, 4570–4577.
10. Choudhury, N.; Pettitt, B. M. On the Mechanism of Hydrophobic Association of Nanoscopic Solutes. *J. Am. Chem. Soc.* **2005**, *127*, 3556–3567.
11. Giovambattista, N.; Rossky, P. J.; Debenedetti, P. G. Phase Transitions Induced by Nanoconfinement in Liquid Water. *Phys. Rev. Lett.* **2009**, *102*, 050603.
12. Bratko, D.; Daub, C. D.; Leung, D.; Luzar, A. Effect of Field Direction on Electrowetting in a Nanopore. *J. Am. Chem. Soc.* **2007**, *129*, 2504–2510.
13. Vaitheeswaran, S.; Yin, H.; Rasaiah, J. C. Water between Plates in the Presence of an Electric Field in an Open System. *J. Phys. Chem. B* **2005**, *109*, 6629–6635.
14. Giovambattista, N.; Debenedetti, P. G.; Rossky, P. J. Effect of Surface Polarity on Water Contact Angle and Interfacial Hydration Structure. *J. Phys. Chem. B* **2007**, *111*, 9581–9587.
15. Park, J. H.; Aluru, N. R. Diffusion of Water Submonolayers on Hydrophilic Surfaces. *Appl. Phys. Lett.* **2008**, *93*, 253104.
16. Wang, C. L.; Lu, H. J.; Wang, Z. G.; Xiu, P.; Zhou, B.; Zuo, G. H.; Wan, R. Z.; Hu, J.; Fang, H. P. Stable Liquid Water Droplet on a Water Monolayer Formed at Room Temperature on Ionic Model Substrates. *Phys. Rev. Lett.* **2009**, *103*, 137801.
17. Koga, K.; Gao, G. T.; Tanaka, H.; Zeng, X. C. Formation of Ordered Ice Nanotubes Inside Carbon Nanotubes. *Nature* **2001**, *412*, 802–805.
18. Bai, J. E.; Wang, J.; Zeng, X. C. Multiwalled Ice Helixes and Ice Nanotubes. *Proc. Natl. Acad. Sci. U.S.A.* **2006**, *103*, 19664–19667.
19. Mashl, R. J.; Joseph, S.; Aluru, N. R.; Jakobsson, E. Anomalously Immobilized Water: A New Water Phase Induced by Confinement in Nanotubes. *Nano Lett.* **2003**, *3*, 589–592.
20. Mikami, F.; Matsuda, K.; Kataura, H; Maniwa, Y. Dielectric Properties of Water Inside Single-Walled Carbon Nanotubes. *ACS Nano* **2009**, *3*, 1279–1287.
21. Thomas, J. A.; McGaughey, A. J. H. Water Flow in Carbon Nanotubes: Transition to Subcontinuum Transport. *Phys. Rev. Lett.* **2009**, *102*, 184502.
22. Duan, W. H.; Wang, Q. Water Transport with a Carbon Nanotube Pump. *ACS Nano* **2010**, *4*, 2338–2344.
23. Mukherjee, B.; Maiti, P. K.; Dasgupta, C.; Sood, A. K. Single-File Diffusion of Water Inside Narrow Carbon Nanorings. *ACS Nano* **2010**, *4*, 985–991.
24. Rasaiah, J. C.; Garde, S.; Hummer, G. Water in Nonpolar Confinement: From Nanotubes to Proteins and Beyond. *Annu. Rev. Phys. Chem.* **2008**, *59*, 713–740.
25. Sholl, D. S.; Johnson, J. K. Making High-Flux Membranes with Carbon Nanotubes. *Science* **2006**, *312*, 1003–1004.
26. Yeh, I. C.; Hummer, G. Nucleic Acid Transport through Carbon Nanotube Membranes. *Proc. Natl. Acad. Sci. U.S.A.* **2004**, *101*, 12171–12182.
27. Gong, X. J.; Li, J. C.; Xu, K.; Wang, J. F.; Yang, H. A Controllable Molecular Sieve for Na^+ and K^+ Ions. *J. Am. Chem. Soc.* **2010**, *132*, 1873–1877.
28. Kalra, A.; Garde, S.; Hummer, G. Osmotic Water Transport through Carbon Nanotube Membranes. *Proc. Natl. Acad. Sci. U.S.A.* **2003**, *100*, 10175–10180.
29. Hummer, G. Water, Proton, and Ion Transport: From Nanotubes to Proteins. *Mol. Phys.* **2007**, *105*, 201–207.
30. Service, R. F. Desalination Freshens Up. *Science* **2006**, *313*, 1088–1090.
31. Corry, B. Designing Carbon Nanotube Membranes for Efficient Water Desalination. *J. Phys. Chem. B* **2008**, *112*, 1427–1434.
32. Dellago, C.; Hummer, G. Kinetics and Mechanism of Proton Transport across Membrane Nanopores. *Phys. Rev. Lett.* **2006**, *97*, 245901.
33. Kreuer, K. D.; Paddison, S. J.; Spohr, E.; Schuster, M. Transport in Proton Conductors for Fuel-Cell Applications Simulations Elementary Reactions and Phenomenology. *Chem. Rev.* **2004**, *104*, 4637–4678.
34. Yuan, Q. Z.; Zhao, Y. P. Hydroelectric Voltage Generation Based on Water-Filled Single-Walled Carbon Nanotubes. *J. Am. Chem. Soc.* **2009**, *131*, 6374–6376.
35. Zhao, Y. C.; Song, L.; Deng, K.; Liu, Z.; Zhang, Z. X.; Yang, Y. L.; Wang, C.; Yang, H. F.; Jin, A. Z.; Luo, Q.; *et al.* Individual Water-Filled Single-Walled Carbon Nanotubes as Hydroelectric Power Converters. *Adv. Mater.* **2008**, *20*, 1772–1776.
36. Bhirde, A. A.; Patel, V.; Gavard, J.; Zhang, G. F.; Sousa, A. A.; Masedunskas, A.; Leapman, R. D.; Weigert, R.; Gutkind, J. S.; Rusling, J. F. Targeted Killing of Cancer Cells *In Vivo* and *In Vitro* with EGF-Directed Carbon Nanotube-Based Drug Delivery. *ACS Nano* **2009**, *3*, 307–316.
37. Bianco, A.; Kostarelos, K.; Prato, M. Applications of Carbon Nanotubes in Drug Delivery. *Curr. Opin. Chem. Biol.* **2005**, *9*, 674–679.
38. Javey, A. The 2008 Kavli Prize in Nanoscience: Carbon Nanotubes. *ACS Nano* **2008**, *2*, 1329–1335.
39. Tu, Y. S.; Xiu, P.; Wan, R. Z.; Hu, J.; Zhou, R. H.; Fang, H. P. Water-Mediated Signal Multiplication with Y-Shaped Carbon Nanotubes. *Proc. Natl. Acad. Sci. U.S.A.* **2009**, *106*, 18120–18124.
40. Ghosh, S; Sood, A. K.; Kumar, N. Carbon Nanotube Flow Sensors. *Science* **2003**, *299*, 1042–1044.
41. Fang, H. P.; Wan, R. Z.; Gong, X. J.; Lu, H. J.; Li, S. Y. Dynamics of Single-File Water Chains Inside Nanoscale Channels: Physics, Biological Significance and Applications. *J. Phys. D: Appl. Phys.* **2008**, *41*, 103002.
42. Preston, G, M.; Agre, P. Isolation of the cDNA for Erythrocyte Integral Membrane Protein of 28 Kilodaltons: Member of an Ancient Channel Family. *Proc. Natl. Acad. Sci. U.S.A.* **1991**, *88*, 11110–11114.
43. Murata, K.; Mitsuoka, K.; Hirai, T.; Walz, T.; Agre, P.; Heymann, J. B.; Engel, A.; Fujiyoshi, Y. Structural Determinants of Water Permeation through Aquaporin-1. *Nature* **2000**, *407*, 599–605.
44. Agre, P. Aquaporin Water Channels (Nobel Lecture). *Angew. Chem., Int. Ed.* **2004**, *43*, 4278–4290.
45. Liu, H. T.; He, J.; Tang, J. Y.; Liu, H; Pang, P.; Cao, D.; Krstic, P.; Joseph, S.; Lindsay, S.; Nuckolls, C. Translocation of Single-Stranded DNA through Single-Walled Carbon Nanotubes. *Science* **2010**, *327*, 64–67.
46. Miyazawa, A.; Fujiyoshi, Y; Unwin, N. Structure and Gating Mechanism of the Acetylcholine Receptor Pore. *Nature* **2003**, *423*, 949–955.
47. Sui, H, X.; Han, B. G.; Lee, J. K.; Walian, P.; Jap, B. K.

Structural Basis of Water Specific Transport through the AQP1 Water Channel. *Nature* **2001**, *414*, 872–878.
48. De Groot, B. L.; Grubmuller, H. Water Permeation across Biological Membranes: Mechanism and Dynamics of Aquaporin-1 and GlpF. *Science* **2001**, *294*, 2353–2357.
49. Zhu, F. Q.; Tajkhorshid, E.; Schulten, K. Pressure-Induced Water Transport in Membrane Channels Studied by Molecular Dynamics. *Biophys. J.* **2002**, *83*, 154–160.
50. Zhu, F. Q.; Tajkhorshid, E.; Schulten, K. Theory and Simulation of Water Permeation in Aquaporin-1. *Biophys. J.* **2004**, *86*, 50–57.
51. Hummer, G.; Rasaiah, J. C.; Noworyta, J. P. Water Conduction through the Hydrophobic Channel of a Carbon Nanotube. *Nature* **2001**, *414*, 188–190.
52. Waghe, A.; Rasaiah, J. C.; Hummer, G. Filling and Emptying Kinetics of Carbon Nanotubes in Water. *J. Chem. Phys.* **2002**, *117*, 10789–10795.
53. Holt, J. K.; Gyu Park, H.; Wang, Y. M.; Stadermann, M.; Artyukhin, A. B.; Grigoropoulos, C. P.; Noy, A.; Bakajin, O. Fast Mass Transport through Sub-2-Nanometer Carbon Nanotubes. *Science* **2006**, *312*, 1034–1037.
54. Joseph, S.; Aluru, N. R. Why are Carbon Nanotubes Fast Transporters of Water? *Nano Lett.* **2008**, *8*, 452–458.
55. Li, J. Y.; Gong, X. J.; Lu, H. J.; Li, D.; Fang, H. P.; Zhou, R. H. Electrostatic Gating of a Nanometer Water Channel. *Proc. Natl. Acad. Sci. U.S.A.* **2007**, *104*, 3687–3692.
56. Wan, R. Z.; Li, J. Y.; Lu, H. J.; Fang, H. P. Controllable Water Channel Gating of Nanometer Dimensions. *J. Am. Chem. Soc.* **2005**, *127*, 7166–7170.
57. Raghunathan, A. V.; Aluru, N. R. Molecular Understanding of Osmosis in Semipermeable Membranes. *Phys. Rev. Lett.* **2006**, *97*, 024501.
58. Suk, M. E.; Aluru, A. R. Effect of Induced Electric Field on Single-File Reverse Osmosis. *Phys. Chem. Chem. Phys.* **2009**, *11*, 8614–8619.
59. Suk, M. E.; Raghunathan, A. V.; Aluru, N. R. Fast Reverse Osmosis Using Boron Nitride and Carbon Nanotubes. *Appl. Phys. Lett.* **2008**, *92*, 133120.
60. Gong, X. J.; Li, J. Y.; Lu, H. J.; Wan, R. Z.; Li, J. C.; Hu, J.; Fang, H. P. A Charge Driven Molecular Water Pump. *Nat. Nanotechnol.* **2007**, *2*, 709–712.
61. Zuo, G. C.; Shen, R.; Ma, S. J.; Guo, W. L. Transport Properties of Single-File Water Molecules Inside a Carbon Nanotube Biomimicking Water Channel. *ACS Nano* **2010**, *4*, 205–210.
62. Wan, R. Z.; Lu, H. J.; Li, J. Y.; Bao, J. D.; Hu, J.; Fang, H. P. Concerted Orientation Induced Unidirectional Water Transport through Nanochannels. *Phys. Chem. Chem. Phys.* **2009**, *11*, 9898–9902.
63. Vaitheeswaran, S.; Rasaiah, J. C.; Hummer, G. Electric Field and Temperature Effects on Water in the Narrow Nonpolar Pores of Carbon Nanotubes. *J. Chem. Phys.* **2004**, *121*, 7955–7964.
64. Joseph, S.; Aluru, N. R. Pumping of Confined Water in Carbon Nanotubes by Rotation−Translation Coupling. *Phys. Rev. Lett.* **2008**, *101*, 064502.
65. Shim, B. S.; Tang, Z. Y.; Morabito, M. P.; Agarwal, A.; Hong, H. P.; Kotov, N. A. Integration of Conductivity, Transparency, and Mechanical Strength into Highly Homogeneous Layer-by-Layer Composites of Single-Walled Carbon Nanotubes for Optoelectronics. *Chem. Mater.* **2007**, *19*, 5467–5474.
66. Mamedov, A. A.; Kotov, N. A.; Prato, M.; Guldi, D. M.; Wicksted, J. P.; Hirsch, A. Molecular Design of Strong Single-Wall Carbon Nanotube/Polyelectrolyte Multilayer Composites. *Nat. Mater.* **2002**, *1*, 190–194.
67. Shim, B. S.; Zhu, J.; Jan, E.; Critchley, K.; Ho, S.; Podsiadlo, P.; Sun, K.; Kotov, N. A. Multiparameter Structural Optimization of Single-Walled Carbon Nanotube Composites: Toward Record Strength, Stiffness, and Toughness. *ACS Nano* **2009**, *3*, 1711–1722.
68. Jorgensen, W. L.; Chandrasekhar, J.; Madura, J. D.; Impey, R. W.; Klein, M. L. Comparison of Simple Potential Functions for Simulating Liquid Water. *J. Chem. Phys.* **1983**, *79*, 926–935.
69. Heymann, J. B.; Engel, A. Aquaporins: Phylogeny, Structure, and Physiology of Water Channels. *News. Physiol. Sci.* **1999**, *14*, 187–193.
70. Walz, T.; Smith, B. L.; Zeidel, M.; Engel, A.; Agre, P. Biologically Active Two-Dimensional Crystals of Aquaporin CHIP. *J. Biol. Chem.* **1994**, *269*, 1583–1586.
71. Zhang, Y. B.; Tang, T. T.; Girit, C.; Hao, Z.; Martin, M. C.; Zettl, A.; Crommie, M. F.; Ron, Y.; Shen, Y. R.; Wang, F. Direct Observation of a Widely Tunable Bandgap in Bilayer Grapheme. *Nature* **2009**, *459*, 820–823.
72. Won, C. Y.; Joseph, S.; Aluru, N. R. Effect of Quantum Partial Charges on the Structure and Dynamics of Water in Single-Walled Carbon Nanotubes. *J. Chem. Phys.* **2006**, *125*, 114701.
73. Kofinger, J.; Hummer, G.; Dellago, C. Macroscopically Ordered Water in Nanopores. *Proc. Natl. Acad. Sci. U.S.A.* **2008**, *105*, 13218–13222.
74. Lindahl, E.; Hess, B.; van der Spoel, D. GROMACS 3.0: A Package for Molecular Simulation and Trajectory Analysis. *J. Mol. Model.* **2001**, *7*, 306–317.
75. Essmann, U.; Perera, L.; Berkowitz, M. L.; Darden, T.; Lee, H.; Pedersen, L. G. A Smooth Particle Mesh Ewald Method. *J. Chem. Phys.* **1995**, *103*, 8577–8593.